

A Novel Linear Power Flow Model

Zhentong Shao, *Student Member, IEEE*, Qiaozhu Zhai, *Member, IEEE*, and Xiaohong Guan, *Fellow, IEEE*

Abstract—Linear power flow (LPF) models are important for the solution of large-scale problems in power system analysis. This paper proposes a novel LPF method named data-based LPF (DB-LPF). The DB-LPF is distinct from the data-driven LPF (DD-LPF) model because the DB-LPF formulates the definition set first and then discretizes the set into representative data samples, while the DD-LPF directly mines the variable mappings from historical or measurement data. In this paper, the concept of LPF definition set (i.e., the set where the LPF performs well) is proposed and an analytical algorithm is provided to get the set. Meanwhile, a novel form of AC-PF models is provided, which is helpful in deriving the analytical algorithm and directing the formulations of LPF models. The definition set is discretized by a grid sampling approach and the obtained samples are processed by the least-squares method to formulate the DB-LPF model. Moreover, the model for obtaining the error bound of the DB-LPF is proposed, and the network losses of the DB-LPF is also analyzed. Finally, the DB-LPF model is tested on enormous cases, whose branch parameters are also analyzed. The test results verify the effectiveness and superiority of the proposed method.

Index Terms—Linear power flow model, data-based approach, least-squares, AC power flow model

NOMENCLATURE

k	Index of data samples/scenarios.
N	Total number of system buses.
K	Total number of data samples/scenarios in the data set.
τ	Tap ratio of transformer.
θ_{shift}	Phasor angle shift of transformer or phase shifter.
φ_{ij}	Impedance angle φ of branch (i, j) .
p_{ij} / q_{ij}	Active/Reactive power flow from bus i to bus j .
v_i / θ_i	Voltage magnitude/angle at bus i .
y_{ij} / z_{ij}	Admittance/Impedance of branch (i, j) .
g_{ij} / b_{ij}	Conductance/Susceptance of branch (i, j) .
r_{ij} / x_{ij}	Resistance/Reactance of branch (i, j) .
g_i^{sh} / b_i^{sh}	Shunt conductance/susceptance near bus i .
$\bar{F}_{ij}^p / \bar{F}_{ij}^q$	Active/Reactive power limitation of branch (i, j) .
$\bar{V}_i / \underline{V}_i$	Upper/Lower bound of voltage magnitude at bus i .
$\bar{\theta}_{ij} / \underline{\theta}_{ij}$	Upper/Lower bound of the angle across branch (i, j) .

I. INTRODUCTION

THE power flow model is the basis of power system analysis. The conventional AC power flow model (i.e., AC power flow equations) describe the physical laws of the steady-state AC power grid, and accurately provides the results of active power flow, reactive power flow and voltage. However, the AC power flow (AC-PF) model is mathematically represented as

nonlinear equations, which leads to the non-convexity and high computational burden of optimization problems constrained by AC-PF equations. The non-convexity makes the optimization problems, such as optimal power flow problems, difficult to coverage to the optimal solution [1]. The high computational burden limits the application of AC-PF model in most large-scale and repetitive problems, such as congestion analysis [2], unit commitment [3] and economic dispatch [4]. Therefore, to address the obstacles of AC-PF model, many methods are proposed to give a relaxation or approximation of the nonlinear AC-PF equations, such as the linear approximation methods[5, 6] and the convex relaxation methods[7].

The DC power flow (DC-PF) model is the most widely used linear approximation of the accurate AC-PF model. The classical DC-PF model originates from engineering practice in early days [8] and the term “DC” comes from the assumptions of only lossless MW flows (i.e., active power flows) and nominal voltages. In literature [8], a thoroughly review is given to classify the various DC-PF models into a cold-start type and a hot-start type. The hot-start type DC-PF models correct the approximation errors by adopting preset operating points from the AC-PF model or measurement data [9], while in applications [3, 10] without available operating points, the cold-start type DC-PF models are indispensable. Beyond the classifications in [8], the literature [11] extends the DC-PF model to consider fuzzy-variable-based power injections; literature [12] tries to obtain the error bound of DC-PF model through a convex relaxation approach; literatures [13, 14] focus on the influence of topology on the approximation accuracy of the DC-PF model, and gives a new form of iterative power flow model.

To better improve the approximation accuracy of DC-PF model, the physical-model-based linear power flow (P-LPF) models are proposed [15, 16]. The P-LPF models extend the basic idea of the classical DC-PF model and adopt the techniques of Taylor expansion method. The P-LPF models take into consideration both active and reactive power flow, and introduce voltage magnitude as independent variable. Literature [17] summarizes different types of P-LPF models and proposes a general formulation of the P-LPF models. In literature [18], the truncation error of the general P-LPF model is analyzed. In literature [19, 20], the P-LPF is further improved by expanding the variable space and some views of data-driven methods are absorbed.

Different from the DC-PF models and the P-LPF models, the

This work is supported in part by the National Natural Science Foundation (61773309, 61773308, 11991023, 11991020) of China. (Corresponding author: Qiaozhu Zhai.)

Z. Shao, Q. Zhai, and X. Guan are with Systems Engineering Institute, MOEKLINNS Lab, Xi’an Jiaotong University, Xi’an 710049, China. (e-mail: qzzhai@sei.xjtu.edu.cn).

data-based (or data-driven) power flow (D-LPF) models breaks the limitations of variable space and mappings imposed by the physical model and seek the mappings of power flow variables from historical data or on-line measurement data. Literature [21] proposes a regression-based D-LPF model and uses the partial least-squares to address the data collinearity. Literature [22] proposes an iterative D-LPF approach to linearize the AC-PF equations considering the data noise. Literature [23] proposes a hybrid D-LPF model, in which the data-based regression approach is applied on the approximation errors of the P-LPF models. Literature [24] extends the linear approximation of D-LPF model to the convex approximation, and uses the ensemble learning method to find a quadratic mapping of the power flow variables. In literature [25], the approximation error of the regression-based D-LPF model is bounded through the Rademacher complexity theory, in which the probability distribution is assumed. In literature [26], a theoretical explanation is given to illustrate why the performance of the D-LPF models is much better than the performance of the DC-PF models and the P-LPF models.

Although the above linear power flow models have different formulations, they all reveal a fact that there exists a near linear relationship between the branch MW flow and the phasor angle difference across the branch. Therefore, a natural question is: what is the optimal linear approximation and how can we obtain this approximation?

In this paper, this question is answered systematically on the basis of a DC-PF model (i.e., a novel linear power flow method that only considers MW flow, rather than an extension of the classic DC-PF). The definition of “optimal” as well as the application range of the optimal DC-PF model are defined analytically, and the conditions for the D-LPF model to become the optimal linear power flow model is also pointed out. In fact, this paper answers several essential questions related to the D-LPF models, which are: 1) what kind of data is qualified for obtaining an effective D-LPF model, 2) what range can the D-LPF model be applied and guarantee a high performance, and 3) what is the exact error bound of the D-LPF model under a given application range.

The remainder of the paper is organized as follows: Section II provides the mathematical formulations, which includes the introduction of the previous linear power flow models, and the basic idea, methodology of the optimal DC-PF model. Section III provides case studies and Section IV concludes the paper.

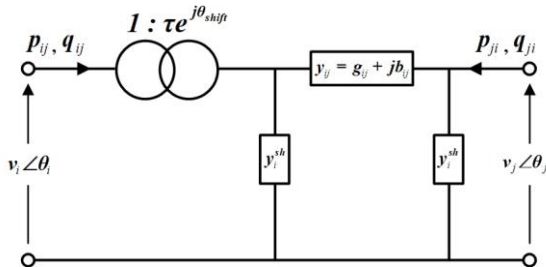


Fig.1 The standard π model for a branch.

II. MATHEMATICAL FORMULATION

In this paper, for all formulations, the phase angles are in radian, and other variables are in per-unit.

A. AC Power Flow Model in Branch Form

The AC-PF model in branch form is provided, which is derived from the detailed transformer-containing form to the common simplified form.

In steady-state power systems, all branches (i.e., including transmission lines, transformers and phase shifters) can be described as a π model shown in Fig. 1, in which the active and reactive power flows of the branch (i, j) are:

$$p_{ij} = -\tau v_i v_j \left[g_{ij} \cos(\theta_{ij} + \theta_{shift}) + b_{ij} \sin(\theta_{ij} + \theta_{shift}) \right] + \tau^2 v_i^2 (g_{ij} + g_i^{sh}), \quad (1)$$

$$q_{ij} = -\tau v_i v_j \left[g_{ij} \sin(\theta_{ij} + \theta_{shift}) - b_{ij} \cos(\theta_{ij} + \theta_{shift}) \right] + \tau^2 v_i^2 (b_i^{sh} - b_{ij}). \quad (2)$$

By equivalently converting the shunt power flows into nodal power injections, the π model can be simplified as the model in Fig. 2, in which the branch active and reactive power flows are:

$$p_{ij} = -v_i' v_j' (g_{ij} \cos \theta_{ij}' + b_{ij} \sin \theta_{ij}') + g_i (v_i')^2, \quad (3)$$

$$q_{ij} = -v_i' v_j' (g_{ij} \sin \theta_{ij}' - b_{ij} \cos \theta_{ij}') - b_i (v_i')^2.$$

$$\text{Where, } v_i' = \tau v_i, \quad \theta_{ij}' = \theta_{ij} + \theta_{shift}. \quad (4)$$

Abusing the notations of v_f' and v_f , θ_{ij}' and θ_{ij} , the branch power flows can be expressed as the common forms:

$$p_{ij} = -v_i v_j (g_{ij} \cos \theta_{ij} + b_{ij} \sin \theta_{ij}) + g v_i^2, \quad (5)$$

$$q_{ij} = -v_i v_j (g_{ij} \sin \theta_{ij} - b_{ij} \cos \theta_{ij}) - b v_i^2.$$

B. Previous Linear Power Flow Models

1) The DC-PF models

The traditional LPF models, i.e., the DC-PF models, can be summarized as the following formulation:

$$p_{ij} = h_{ij} \cdot \theta_{ij} + \alpha_{ij}. \quad (6)$$

The h_{ij} and α_{ij} are constant terms, whose values are case-dependent and empirical. In the classical DC-PF model, it takes:

$$h_{ij} = 1/x_{ij}, \quad \alpha_{ij} = 0. \quad (7)$$

The DC-PF models ignore the reactive power, and detailed review of the DC-PF models is available in literature [8].

2) The P-LPF models

The P-LPF models generally takes the basic ideas of Taylor expansion and adopts part of the assumptions in the DC-PF model. The P-LPF models are able to consider the reactive power and voltage. In Literature [17], various types of P-LPF models are summarized and compared, and the formulations of the best-performing P-LPF model in [17] are as follows:

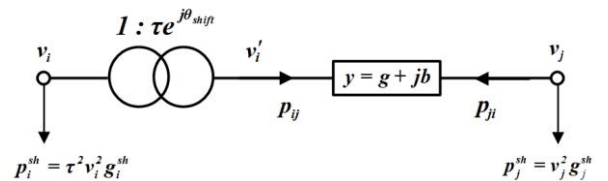


Fig.2 The simplified π model for a branch.

$$p_f = g \frac{v_f^2 - v_i^2}{2} - b \theta + f_{Loss}^p(v_f^2, v_i^2, \theta; v_{f0}^2, v_{i0}^2, \theta_0), \quad (8)$$

$$q_f = -b \frac{v_f^2 - v_i^2}{2} - g \theta + f_{Loss}^q(v_f^2, v_i^2, \theta; v_{f0}^2, v_{i0}^2, \theta_0).$$

Where, $f_{Loss}^p(\cdot)$ and $f_{Loss}^q(\cdot)$ are loss functions who are linear and take (v_f^2, v_i^2, θ) as independent variables and $(v_{f0}^2, v_{i0}^2, \theta_0)$ as parameters (i.e., the initial point for Taylor expansion).

The form of the loss functions indicates that the P-LPF model of (8) works as the hot-start LPF model. When it works as the cold-start model, the loss functions are ignored or simplified to constant parameters. In [17], it is also announced that the P-LPF models can be generalized by expanding the variable space, for example, the $\ln v$ can be regarded as an independent variable to replace the v^2 in (8). More detailed summary of P-LPF models is available in [17].

3) The D-LPF models

The D-LPF models breaks the restriction on the formulation of the physical model and mines the linear relationship between the variables from the data. The formulation of D-LPF models can be summarized as follows:

$$\begin{aligned} p_{ij} &= \alpha^p + \sum_{i=1}^N \beta_i^p v_i + \sum_{i=1}^N \gamma_i^p \theta_i, \\ q_{ij} &= \alpha^q + \sum_{i=1}^N \beta_i^q v_i + \sum_{i=1}^N \gamma_i^q \theta_i. \end{aligned} \quad (9)$$

Where, $\alpha^p, \beta_i^p, \gamma_i^p, \alpha^q, \beta_i^q, \gamma_i^q$ are linear factors that are obtained by applying the linear regression method. The data of the D-LPF models is collected from the historical data or real-time measurement data.

The D-LPF models perform much better than the P-LPF models and DC-PF models. In literature [26], it is explained that the good performance of D-LPF models comes from the fact that the D-LPF models are dedicated to finding the best linear approximation on a regular set (i.e., denoted as *RS*, which is the set defined by the data), and the scenarios in the *RS* appear with high probability in engineering. More detailed summary of the D-LPF models is available in [26].

C. The Definition Set of Linear Power Flow Models.

In our previous literature [26], it proposes a view that a LPF model should be established on a clear definition set. However, the P-LPF models and DC-PF models generally have ambiguous

TABLE I
INFORMATION OF THE EXAMPLE BRANCH

y (p.u.)	g (p.u.)	b (p.u.)	φ (rad)	\bar{F}^p / \bar{F}^q (p.u.)

definition sets, or are basically established on the all-scenarios set (i.e., denoted as *AS*, which contains all scenarios of the original AC-PF model). Since there are many unnecessary low-probability scenarios in *AS*, defining the LPF model on the *AS* obviously sacrifices the accuracy of the model, and it is reasonable to define the LPF model on the *RS*.

The exact formulations of *AS* and *RS* are high-dimensional. Although the high-dimensional *AS* and *RS* successfully define the D-LPF model in [26], the exact *AS* and *RS* are failed to be applied in the quantitative computations.

In this paper, the idea of dimensionality reduction is adopted. For a single branch, it is found that the definition set for the LPF model can be realized by using the following formulations:

$$S^p = \left\{ (p_{ij}, v_i, v_j, \theta_{ij}) \left| \begin{array}{l} p_{ij} = g v_i^2 - v_i v_j (g_{ij} \cos \theta_{ij} + b_{ij} \sin \theta_{ij}), \\ \underline{V}_i \leq v_i \leq \bar{V}_i, \underline{V}_j \leq v_j \leq \bar{V}_j, \\ -\bar{F}_{ij}^p \leq p_{ij} \leq \bar{F}_{ij}^p, \underline{\theta}_{ij}^{\text{Tr}} \leq \theta_{ij} \leq \bar{\theta}_{ij}^{\text{Tr}}. \end{array} \right. \right\} \quad (10)$$

$$S^q = \left\{ (q_{ij}, v_i, v_j, \theta_{ij}) \left| \begin{array}{l} q_{ij} = -b v_i^2 - v_i v_j (g_{ij} \sin \theta_{ij} - b_{ij} \cos \theta_{ij}), \\ \underline{V}_i \leq v_i \leq \bar{V}_i, \underline{V}_j \leq v_j \leq \bar{V}_j, \\ -\bar{F}_{ij}^q \leq q_{ij} \leq \bar{F}_{ij}^q, \underline{\theta}_{ij}^{\text{Tr}} \leq \theta_{ij} \leq \bar{\theta}_{ij}^{\text{Tr}}. \end{array} \right. \right\} \quad (11)$$

It is worth attention that the true boundary of θ (i.e., $\theta \in [\underline{\theta}_{ij}^{\text{Tr}}, \bar{\theta}_{ij}^{\text{Tr}}]$) is used. This is because the initial boundary of θ (i.e., $\theta \in [\underline{\theta}_{ij}, \bar{\theta}_{ij}]$) are estimated and the limitations of branch power flows lead to an implicit boundary of θ (i.e., denoted as $\theta \in [\underline{\theta}_{ij}^{\text{lm}}, \bar{\theta}_{ij}^{\text{lm}}]$). Then the true boundary is obtained by:

$$\underline{\theta}_{ij}^{\text{Tr}} = \max\{\underline{\theta}_{ij}^{\text{lm}}, \underline{\theta}_{ij}\}, \bar{\theta}_{ij}^{\text{Tr}} = \min\{\bar{\theta}_{ij}^{\text{lm}}, \bar{\theta}_{ij}\}. \quad (12)$$

The S^p and S^q are controlled by adjusting the boundary parameters, and the *AS* and *RS* can be obtained by adjusting the sets according to applications.

D. A Novel Form of AC-PF Model

For a given branch, it has:

$$g_{ij} + j b_{ij} = \frac{1}{r_{ij} + j x_{ij}} = \frac{1}{z_{ij} e^{j \varphi_{ij}}} = y_{ij} e^{-j \varphi_{ij}} \quad (13)$$

Then, it can be obtained:

$$g_{ij} = y_{ij} \cos \varphi_{ij}, b_{ij} = -y_{ij} \sin \varphi_{ij}, \varphi_{ij} = \arctan(-b_{ij} / g_{ij}) \quad (14)$$

By substituting (14) into the branch active power flow model in the formulation (5), it has:

$$\begin{aligned} p_{ij} &= g_{ij} v_i^2 - v_i v_j (y_{ij} \cos \varphi_{ij} \cos \theta_{ij} - y_{ij} \sin \varphi_{ij} \sin \theta_{ij}) \\ &\Downarrow \\ p_{ij} &= g_{ij} v_i^2 - v_i v_j y_{ij} (\cos \varphi_{ij} \cos \theta_{ij} - \sin \varphi_{ij} \sin \theta_{ij}) \quad (15) \\ &\Downarrow \end{aligned}$$

$$p_{ij} = g_{ij} v_i^2 - v_i v_j y_{ij} \cos(\theta_{ij} + \varphi_{ij})$$

Then, the novel form of the AC-PF model is:

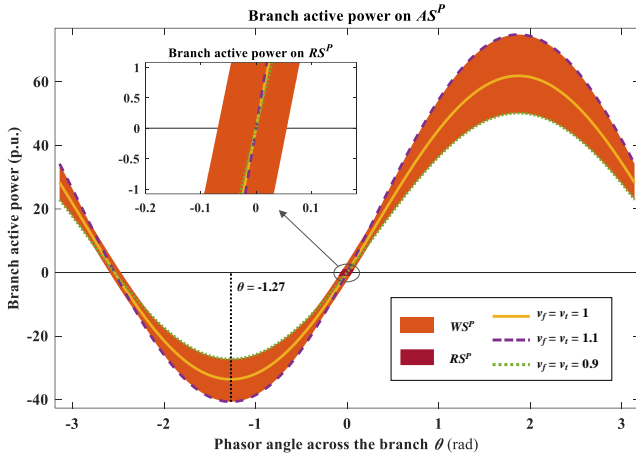
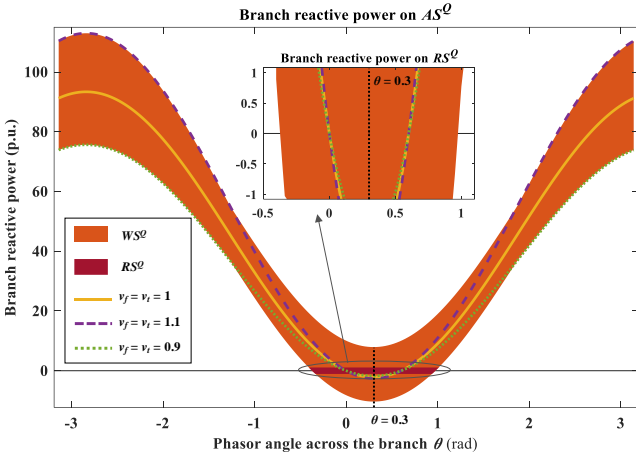
$$p_{ij} = g_{ij} v_i^2 - v_i v_j y_{ij} \cos(\theta_{ij} + \varphi_{ij}), \quad (16)$$

$$q_{ij} = -b_{ij} v_i^2 - v_i v_j y_{ij} \sin(\theta_{ij} + \varphi_{ij}). \quad (17)$$

The novel form can help us to explain the characteristics of the AC-PF model and show the situations that the AC-PF can

TABLE II
PARAMETERS OF THE DEFINITION SETS

Sets	Parameters
AS^p	$v_f, v_i \in [0.9, 1.1], p_f \in (-\infty, +\infty), \theta \in [-\pi, \pi]$.
RS^p	$v_f, v_i \in [0.9, 1.1], p_f \in (-1.08, 1.08), \theta \in [-\pi/3, \pi/3]$.
AS^q	$v_f, v_i \in [0.9, 1.1], q_f \in (-\infty, +\infty), \theta \in [-\pi, \pi]$.
RS^q	$v_f, v_i \in [0.9, 1.1], q_f \in (-1.08, 1.08), \theta \in [-\pi/3, \pi/3]$.

Fig.3 Branch active power on AS^P and RS^P .Fig.4 Branch reactive power on AS^Q and RS^Q (Reactive Power).

be well approximated by a linear function. To better illustrate the ideas, and example is given, the parameters of the example branch are given in the Table I, and the parameters of the AS and RS used for the examples are shown in Table II.

With the novel AC-PF form, it focuses on the plane of P_{ij}/Q_{ij} versus θ . With a fixed v_f and v_i , it obtains a sine/cosine-like curve on the plane, and with all v_f and v_i in the AS/RS, the infinite curves are superimposed into an area. The areas of the example branch are depicted in Fig. 4 and Fig. 5, in which the difference between AS and RS is shown concretely.

From the Fig. 3, it can be found that:

a) The p_{ij} is a cosine function versus θ_{ij} , and the function is stretched and translated by the voltages. The p_{ij} is monotonic versus θ_{ij} on RS (i.e., it is even monotonic on a wide range of $\theta \in [-\varphi, \pi - \varphi]$), which makes it possible to use a single-piece linear function to approximate the p_{ij} appropriately.

b) By imposing the power flow limitations, the AC-PF model will be limited to a relatively small set (i.e., the RS). Within this small set, the AC-PF is quite close to linear function. The RS is much smaller than the AS. The true range of θ is $[-0.096, 0.078]$, which is much smaller than the initial range of $\theta \in [-\pi/3, \pi/3]$. The true range of θ is near zero.

From the Fig. 4, it can be found that:

a) The q_{ij} is not monotonic versus θ_{ij} on RS (i.e., it is even not monotonic on a wide range of $\theta \in [-\pi/2, \pi/2]$), which

TABLE III
PARTIAL DERIVATIVES BASED ON THE NOVEL AC-PF FORM

Derivatives	P_{ij} versus θ_{ij}	Q_{ij} versus θ_{ij}
First-order	$v_i v_j y_{ij} \sin(\theta_{ij} + \varphi_{ij})$	$-v_i v_j y_{ij} \cos(\theta_{ij} + \varphi_{ij})$
Second-order	$v_i v_j y_{ij} \cos(\theta_{ij} + \varphi_{ij})$	$v_i v_j y_{ij} \sin(\theta_{ij} + \varphi_{ij})$
Derivatives	P_{ij} versus v_i	Q_{ij} versus v_i
First-order	$2g_{ij}v_i - v_j y_{ij} \cos(\theta_{ij} + \varphi_{ij})$	$-2b_{ij}v_i - v_j y_{ij} \sin(\theta_{ij} + \varphi_{ij})$
Second-order	$2g_{ij}$	$-2b_{ij}$
Derivatives	P_{ij} versus v_j	Q_{ij} versus v_j
First-order	$-v_i y_{ij} \cos(\theta_{ij} + \varphi_{ij})$	$-v_i y_{ij} \sin(\theta_{ij} + \varphi_{ij})$
Second-order	0	0

TABLE IV
ESTIMATED PARTIAL DERIVATIVES UNDER THE ASSUMPTIONS

Assumptions:	$\varphi: \pi/4 \rightarrow \pi/2$	$\theta_{ij} \approx 0, v_i, v_j \in [0.9, 1.1]$
Derivatives	P_{ij} versus θ_{ij}	Q_{ij} versus θ_{ij}
First-order	$0.7v_i v_j y_{ij} \rightarrow v_i v_j y_{ij}$	$-0.7y_{ij} \rightarrow 0$
Second-order	$0.7y_{ij} \rightarrow 0$	$0.7y_{ij} \rightarrow y_{ij}$
Derivatives	P_{ij} versus v_i	Q_{ij} versus v_i
First-order	$2g_{ij} - 0.7y_{ij} \rightarrow 2g_{ij}$	$-2b_{ij} - 0.7y_{ij} \rightarrow -2b_{ij} - y_{ij}$
Second-order	$2g_{ij}$	$-2b_{ij}$
Derivatives	P_{ij} versus v_j	Q_{ij} versus v_j
First-order	$-0.7y_{ij} \rightarrow 0$	$-0.7y_{ij} \rightarrow -y_{ij}$
Second-order	0	0

makes it hard to approximate the q_{ij} by a single-piece linear function. the symmetry axis of $\theta = 0.3$ comes from:

$$\theta = -\varphi + \pi/2 \approx -1.27 + 1.57 = 0.3 \quad (18)$$

b) The RS of reactive power is also smaller than the AS. The implicit range of θ (i.e., $\theta \in [-0.42, 1.02]$) is close to the initial range of $\theta \in [-\pi/3, \pi/3]$.

In general, the smaller the change of the first-order derivative in function, and the closer the second-order derivative function is to zero, the better the function can be linearized.

With the novel AC-PF form, partial derivatives of P_{ij} and Q_{ij} are given in the Table III. By taking some assumptions in DC-PF, the value of the derivatives can be estimated in the Table IV.

a) Both the first- and second-order derivatives of P_{ij}/Q_{ij} versus θ_{ij}

The above analysis gives two conclusion that 1) the active power of AC-PF model can be approximated by linear function, while the reactive power of AC-PF model is difficult to be approximated linearly; 2) it is reasonable to seek the best linear approximation on RS than AS.

E. The Methodology for Obtaining the Novel LPF Model

1) The Formulation of the Novel LPF Model

Based on the above basic ideas, the monotonicity of the AC-PF on RS is discussed first.

Active power flow: since the $x/r \geq 1$ occurs for almost all branches in engineering, and the AC-PF of active power is monotonic on $\theta \in [-\varphi, \pi - \varphi]$, it has $\varphi \in (\pi/4, \pi/2]$ and the AC-PF of active power is monotonic on $\theta \in [-\pi/4, \pi/4]$, which is a wide enough range for most engineering applications.

The above discussion shows that the single-piece linear approximation is applicable for active power, which is consistent with the experience of DC-PF, P-LPF and D-LPF models.

Accordingly, the active power flow is approximate by the following formulation:

$$P_f^{LPP} = \alpha^P + \beta_f^P v_f + \beta_i^P v_i + \gamma^P \theta \quad (19)$$

Reactive power flow: the AC-PF of reactive power is monotonic on the formulation (20).

$$\theta \in [-\frac{\pi}{2} - \varphi, \frac{\pi}{2} - \varphi] \cup [\frac{\pi}{2} - \varphi, \frac{3\pi}{2} - \varphi] \quad (20)$$

Since the $\varphi \in (\pi/4, \pi/2]$, the symmetry axis $\theta^s = \pi/2 - \varphi$ is always within $[-\pi/4, \pi/4]$. Therefore, the AC-PF of active power flow should be approximated by double-piece linear functions, which can be expressed as follows:

$$q_f^{LPP} = \alpha^Q + \beta_f^Q v_f + \beta_i^Q v_i + \gamma^Q \hat{\theta}, \quad (21)$$

$$\text{Where, } \hat{\theta} = \begin{cases} \theta, & \theta \in [\theta^s, \bar{\theta}] \\ 2\theta^s - \theta, & \theta \in [\underline{\theta}, \theta^s] \end{cases} \quad (22)$$

Where, the formulation (22) actually uses the symmetry of the two pieces linear approximation functions.

Afterwards, the formulas in (22) are spliced through the formula in mixed-integer linear programming, which is shown as follows:

2) The Grid Sampling Algorithm

To obtain the linear factors in formulations (19) and (21), the *RS* is discretized by a grid sampling algorithm.

Algorithm: Grid Sampling

Step 1: (Initialization) Set the sampling number M and N , and generate $v_f^{(m)}, v_i^{(m)}, \theta^{(n)}$ by (23)-(25) as follows:

$$v_f^{(i)} = \underline{V}_f + [(\bar{V}_f - \underline{V}_f)(i-1)] / (M-1), \forall i = 1, 2, \dots, M \quad (23)$$

$$v_i^{(j)} = \underline{V}_i + [(\bar{V}_i - \underline{V}_i)(j-1)] / (M-1), \forall j = 1, 2, \dots, M \quad (24)$$

$$\theta^{(n)} = \underline{\theta}^{\text{Tr}} + [(\bar{\theta}^{\text{Tr}} - \underline{\theta}^{\text{Tr}})(n-1)] / (M-1), \forall n = 1, 2, \dots, N \quad (25)$$

Step 2: (Sampling) Set $k = 0$ and initialize $RS = \emptyset$. Then do the following algorithm:

For i from 1 to M ,

For j from 1 to M ,

For n from 1 to N ,

Calculate p_f by:

$$p_f = g v_f^{(i)} (v_f^{(i)} - v_i^{(j)} \cos \theta^{(n)}) - v_f^{(i)} v_i^{(j)} b \sin \theta^{(n)};$$

If $-\bar{F} \leq p_f \leq \bar{F}$,

save p_f to RS , $k = k+1$;

End if.

End for.

End for.

End for.

Save the maximum k as K .

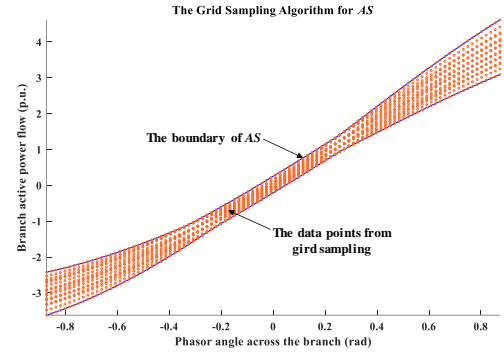


Fig.5 The performance of grid sampling algorithm on AS.

It is worth attention that the formulation (25) uses the true range of θ (i.e., $\theta \in [\underline{\theta}^{\text{Tr}}, \bar{\theta}^{\text{Tr}}]$). This is because the enforcement of power flow limitations leads to an implicit range of θ (i.e., $\theta \in [\underline{\theta}^{\text{Im}}, \bar{\theta}^{\text{Im}}]$). The true range is obtained by:

$$\underline{\theta}^{\text{Tr}} = \max\{\underline{\theta}^{\text{Im}}, \underline{\theta}\}; \quad \bar{\theta}^{\text{Tr}} = \min\{\bar{\theta}^{\text{Im}}, \bar{\theta}\}. \quad (26)$$

Where, the $[\underline{\theta}, \bar{\theta}]$ is the given range in the *RS*. Further, the $[\underline{\theta}^{\text{Im}}, \bar{\theta}^{\text{Im}}]$ is obtained by solving the following problems:

$$\bar{\theta}^{\text{Im}} = \max \theta$$

$$\text{s.t. } \bar{F} = g v_f (v_f - v_i \cos \theta) - v_f v_i b \sin \theta \quad (27)$$

$$\underline{V}_f \leq v_f \leq \bar{V}_f, \quad \underline{V}_i \leq v_i \leq \bar{V}_i$$

$$\underline{\theta}^{\text{Im}} = \min \theta$$

$$\text{s.t. } -\bar{F} = g v_f (v_f - v_i \cos \theta) - v_f v_i b \sin \theta \quad (28)$$

$$\underline{V}_f \leq v_f \leq \bar{V}_f, \quad \underline{V}_i \leq v_i \leq \bar{V}_i$$

The interior point method is used to solve the problems (27) and (28). The solution of interior point method is fast, but it cannot guarantee a global optimum since the problems (27) and (28) are non-convex. Considering that the role of $[\underline{\theta}^{\text{Im}}, \bar{\theta}^{\text{Im}}]$ is to reduce the range of θ and to improve the sampling accuracy, the values of $\underline{\theta}^{\text{Im}}, \bar{\theta}^{\text{Im}}$ do not need to be accurate, therefore, the following formulations are used to corrected the solutions (i.e., denoted as $\underline{\theta}^{\text{Im}*}, \bar{\theta}^{\text{Im}*}$) obtained by the interior point method:

$$\underline{\theta}^{\text{Im}} = \underline{\theta}^{\text{Im}*} - |\eta \underline{\theta}^{\text{Im}*}|, \quad \bar{\theta}^{\text{Im}} = \bar{\theta}^{\text{Im}*} + |\eta \bar{\theta}^{\text{Im}*}|. \quad (29)$$

Where, η is a heuristic parameter. Empirically, $\eta = 15\%$. An example is given in Fig. 5 to show the performance of the grid sampling algorithm.

Compared with the high-dimensional historical or measurement samples in D-LPF models, the samples obtained by the grid sampling algorithm have three advantages:

1) The sampling accuracy is controllable.

2) The samples are sufficient (i.e., as shown in Fig. 5), and there is no need to add artificial assumptions due to the data is insufficient or not representative.

3) The samples have no troubles with the data collinearity and data noise.

3) The Problem for Obtaining the Novel LPF Model

The novel LPF models under two metrics are provided, the metrics are:

- **LS:** The sum of the squares of the approximation errors of all points in the *RS* is minimized, i.e., the least-squares.

- **Min-Max:** The maximum absolute approximation error of all points in the RS is minimized, i.e., the best uniform approximation.

The metric of **LS** is adopted in D-LPF models, and the metric of **Min-Max** is given in this paper to compare the common used metric of **LS**.

Let $RS(K)$ be the discretized RS that contains K samples. The optimization problems for obtaining the linear factors of the novel LPF model of active power are described as follows:

a) *The problem for active power with metric of LS.*

(P-LS)

$$\begin{aligned} \min_{\alpha^p, \beta_f^p, \beta_i^p, \gamma^p} & \sum_{k=1}^K (p_f^{LPF, (k)} - p_f^{AC, (k)})^2 \\ \text{s.t. } & p_f^{LPF, (k)} = \alpha^p + \beta_f^p v_f^{(k)} + \beta_i^p v_i^{(k)} + \gamma^p \theta^{(k)} \\ & p_f^{(k)}, v_f^{(k)}, v_i^{(k)}, \theta^{(k)} \in RS(K) \end{aligned} \quad (30)$$

b) *The problem for reactive power with metric of LS.*

The RS of reactive power is divided into two parts by the axis of symmetry, that is, $[\theta, \theta]$

and we discretize the larger part of it as RSK

(Q-LS)

b) *The problem with metric of Min-Max.*

(P-MinMax)

$$\begin{aligned} \min_{\alpha^p, \beta_f^p, \beta_i^p, \gamma^p} & \beta \\ \text{s.t. } & -\beta \leq p_f^{LPF, (k)} - p_f^{(k)} \leq \beta \\ & p_f^{LPF, (k)} = \alpha^p + \beta_f^p v_f^{(k)} + \beta_i^p v_i^{(k)} + \gamma^p \theta^{(k)} \\ & p_f^{(k)}, v_f^{(k)}, v_i^{(k)}, \theta^{(k)} \in RS(K) \end{aligned} \quad (31)$$

Where, β is an auxiliary variable.

The **P-LS** can be solved analytically by the complete orthogonal decomposition approach in [26]. The **P-MinMax** is a linear programming problem, which can be solved efficiently by commercial solvers.

F. The Error Bound of the Novel LPF Model

After obtaining the optimal DC-PF model, a verification step is needed, that is, obtaining the exact error bound of the optimal DC-PF model within the specified range. This verification is completed by the following programming problem:

$$\max_{\theta, v_f, v_i} E = |p_f - p_f^{AC}| \quad (32)$$

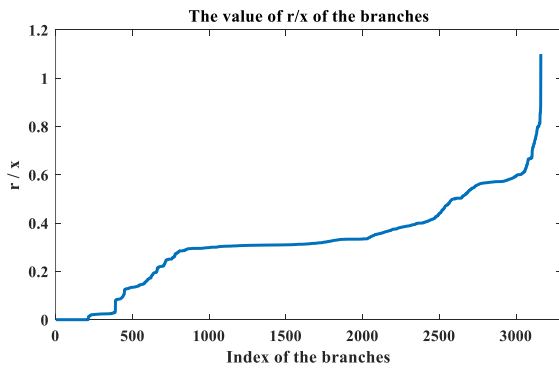


Fig.6 The r/x values of the branches

G. Flowchart

The flowchart of the optimal DC-PF method is given in the Fig. 10.

III. CASE STUDY

A. Configurations

The approximate performance and computational efficiency of the optimal DC-PF model are not related to the scale of the system, and the most crucial factor that influence the performance of the optimal DC-PF model is the r/x ratio of the branch. Therefore, the branches of IEEE 24-bus system, 30-bus system, 118-bus system and 2383-bus system are gathered and sorted by the value of r/x . The r/x of the branches are shown in the Fig. 12, in which there are 3161 branches.

The test systems are from MATPOWER 7.1 [27], and the code is performed with MATLAB 2019R on a computer of Intel Core i7-4790 CPU @ 3.60 GHz, 28 GB RAM.

The case study is aims to answer the following questions:

- The impact of M, N of the grid sampling method to the approximation accuracy and computational time of the optimal DC-PF model.
- The impact of r/x on the optimal DC-PF model.
- The performance of branch loss approximation.
- The comparison of the metrics of the optimal DC-PF model.

B. The impact of the choice of M, N

First, the impact of M is tested, and the N is fixed as a value of 50. The test range of the branches is set as the formulation (33). Only from-end of the branches are considered in the test.

$$AR = \left\{ \begin{array}{l} p_f = g_i v_f (v_f - v_i \cos \theta) - v_f v_i b_i \sin \theta, \\ 0.95 \leq v_f, v_i \leq 1.05, -2 \leq p_f \leq 2, \\ -0.873 \leq \theta \leq 0.873. \end{array} \right\}, \forall l \quad (33)$$

The approximation accuracy and computational time are tested with different set of M and N , the results are given in the Fig. 6 and Fig. 7.

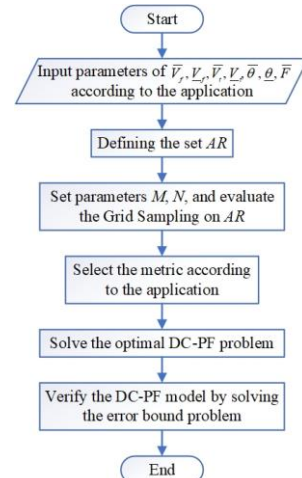


Fig.7 The flowchart of optimal DC-PF method.

REFERENCES

- [1] A. Nasri, S. J. Kazempour, A. J. Conejo, and M. Ghandhari, "Network-Constrained AC Unit Commitment Under Uncertainty: A Benders' Decomposition Approach," *IEEE Transactions on Power Systems*, vol. 31, no. 1, pp. 412-422, 2016.
- [2] P. J. Martínez-Lacañina, A. M. Marcolini, and J. L. Martínez-Ramos, "DCOPF contingency analysis including phase shifting transformers," in *2014 Power Systems Computation Conference*, 2014, pp. 1-7.
- [3] M. Carrion and J. M. Arroyo, "A computationally efficient mixed-integer linear formulation for the thermal unit commitment problem," *IEEE Transactions on Power Systems*, vol. 21, no. 3, pp. 1371-1378, 2006.
- [4] K. E. V. Horn, A. D. Domínguez-García, and P. W. Sauer, "Measurement-Based Real-Time Security-Constrained Economic Dispatch," *IEEE Transactions on Power Systems*, vol. 31, no. 5, pp. 3548-3560, 2016.
- [5] S. Misra, D. K. Molzahn, and K. Dvijotham, "Optimal Adaptive Linearizations of the AC Power Flow Equations," in *2018 Power Systems Computation Conference (PSCC)*, 2018, pp. 1-7.
- [6] T. Mühlpfordt, V. Hagenmeyer, D. K. Molzahn, and S. Misra, "Optimal Adaptive Power Flow Linearizations: Expected Error Minimization using Polynomial Chaos Expansion," in *2019 IEEE Milan PowerTech*, 2019, pp. 1-6.
- [7] J. Lavaei and S. H. Low, "Zero Duality Gap in Optimal Power Flow Problem," (in English), *Ieee Transactions on Power Systems*, vol. 27, no. 1, pp. 92-107, Feb 2012.
- [8] B. Stott, J. Jardim, and O. Alsac, "DC Power Flow Revisited," (in English), *Ieee Transactions on Power Systems*, vol. 24, no. 3, pp. 1290-1300, Aug 2009.
- [9] S. Hossain-McKenzie, S. Etigowni, K. Davis, and S. Zonouz, "Augmented DC power flow method with real-time measurements," in *2016 Power Systems Computation Conference (PSCC)*, 2016, pp. 1-7.
- [10] H. Zhang, G. T. Heydt, V. Vittal, and J. Quintero, "An Improved Network Model for Transmission Expansion Planning Considering Reactive Power and Network Losses," *IEEE Transactions on Power Systems*, vol. 28, no. 3, pp. 3471-3479, 2013.
- [11] H. Livani, S. Jafarzadeh, and M. S. Fadali, "DC power flow using fuzzy linear equations," in *2015 IEEE Power & Energy Society General Meeting*, 2015, pp. 1-5.
- [12] K. Dvijotham and D. K. Molzahn, "Error Bounds on the DC Power Flow Approximation: A Convex Relaxation Approach," (in English), *2016 Ieee 55th Conference on Decision and Control (Cdc)*, pp. 2411-2418, 2016.
- [13] J. W. Simpson-Porco, "Lossy DC Power Flow," *IEEE Transactions on Power Systems*, vol. 33, no. 3, pp. 2477-2485, 2018.
- [14] J. W. Simpson-Porco, "A Theory of Solvability for Lossless Power Flow Equations—Part I: Fixed-Point Power Flow," *IEEE Transactions on Control of Network Systems*, vol. 5, no. 3, pp. 1361-1372, 2018.
- [15] Z. Yang, H. Zhong, A. Bose, T. Zheng, Q. Xia, and C. Kang, "A Linearized OPF Model With Reactive Power and Voltage Magnitude: A Pathway to Improve the MW-Only DC OPF," *IEEE Transactions on Power Systems*, vol. 33, no. 2, pp. 1734-1745, 2018.
- [16] J. W. Yang, N. Zhang, C. Q. Kang, and Q. Xia, "A State-Independent Linear Power Flow Model With Accurate Estimation of Voltage Magnitude," (in English), *Ieee Transactions on Power Systems*, vol. 32, no. 5, pp. 3607-3617, Sep 2017.
- [17] Z. Yang, K. Xie, J. Yu, H. Zhong, N. Zhang, and Q. X. Xia, "A General Formulation of Linear Power Flow Models: Basic Theory and Error Analysis," *IEEE Transactions on Power Systems*, vol. 34, no. 2, pp. 1315-1324, 2019.
- [18] Z. Fan, Z. Yang, H. Jiang, J. Yu, J. Long, and L. Jin, "Truncation Error Analysis of Linear Power Flow Model," in *2020 IEEE Sustainable Power and Energy Conference (iSPEC)*, 2020, pp. 301-306.
- [19] Z. Fan, Z. Yang, J. Yu, K. Xie, and G. Yang, "Minimize Linearization Error of Power Flow Model Based on Optimal Selection of Variable Space," *IEEE Transactions on Power Systems*, vol. 36, no. 2, pp. 1130-1140, 2021.
- [20] J. Long, W. Jiang, L. Jin, T. Zhang, H. Jiang, and T. Xu, "A Combination of Linear Power Flow Models to Reduce Linearization Error," in *2020 IEEE 3rd International Conference of Safe Production and Informatization (IICSPI)*, 2020, pp. 256-260.
- [21] Y. X. Liu, N. Zhang, Y. Wang, J. W. Yang, and C. Q. Kang, "Data-Driven Power Flow Linearization: A Regression Approach," (in English), *Ieee Transactions on Smart Grid*, vol. 10, no. 3, pp. 2569-2580, May 2019.
- [22] Y. Liu, Y. Wang, N. Zhang, D. Lu, and C. Kang, "A Data-Driven Approach to Linearize Power Flow Equations Considering Measurement Noise," *IEEE Transactions on Smart Grid*, vol. 11, no. 3, pp. 2576-2587, 2020.
- [23] Y. Tan, Y. Chen, Y. Li, and Y. Cao, "Linearizing Power Flow Model: A Hybrid Physical Model-Driven and Data-Driven Approach," *IEEE Transactions on Power Systems*, vol. 35, no. 3, pp. 2475-2478, 2020.
- [24] R. Hu, Q. Li, and F. Qiu, "Ensemble Learning Based Convex Approximation of Three-Phase Power Flow," *IEEE Transactions on Power Systems*, vol. 36, no. 5, pp. 4042-4051, 2021.
- [25] Y. Liu, B. Xu, A. Botterud, N. Zhang, and C. Kang, "Bounding Regression Errors in Data-Driven Power Grid Steady-State Models," *IEEE Transactions on Power Systems*, vol. 36, no. 2, pp. 1023-1033, 2021.
- [26] Z. Shao, Q. Zhai, J. Wu, and X. Guan, "Data Based Linear Power Flow Model: Investigation of a Least-Squares Based Approximation," *IEEE Transactions on Power Systems*, vol. 36, no. 5, pp. 4246-4258, 2021.

- [27] R. D. Zimmerman, C. E. Murillo-Sánchez, and R. J. Thomas, "MATPOWER: Steady-State Operations, Planning, and Analysis Tools for Power Systems Research and Education," *IEEE Transactions on Power Systems*, vol. 26, no. 1, pp. 12-19, 2011.